Production of meloxicam suspension using pulsed laser ablation in liquid (PLAL) technique

Béla Hopp[1,*] Eszter Nagy[1] Franciska Peták[1] Tomi Smausz[2,1] Judit Kopniczky[1] Csaba Tápai[1] Judit Budai[1,3] Ibolya Zita Papp[4] Ákos Kukovecz[4] Rita Ambrus[5] and Piroska Szabó-Révész[5]

[1]Department of Optics and Quantum Electronics, University of Szeged, H-6720 Szeged, Dóm tér 9, Hungary

[2]MTA-SZTE Research Group on Photoacoustic Spectroscopy, University of Szeged, 6720 Szeged, Dóm tér 9, Hungary

[3]Attosecond Light Pulse Source, ELI-Hu Nkft, Szeged H-6720, Dugonics tér 13, Hungary

[4]Department of Applied and Environmental Chemistry, University of Szeged, H-6720 Szeged, Rerrich Béla tér 1, Hungary

[5]Institute of Pharmaceutical Technology and Regulatory Affairs, University of Szeged, H-6720 Szeged, Eötvös utca 6, Hungary

[*]Corresponding author: bhopp@physx.u-szeged.hu

Abstract

Production of organic particles in the micrometer/nanometer range can find applications in a wide range of areas, however for a number of materials it is not a straightforward task. In the present work pulsed laser ablation in liquid environment (PLAL) of meloxicam was studied aiming the production of near micrometer sized particles of this pharmaceutical ingredient. Targets pressed from crystalline meloxicam powder were placed in distilled water and irradiated with a focused beam of a frequency doubled (532 nm) nanosecond Nd:YAG laser at 4.2 – 9.4 J/cm^2 fluence. Morphological investigation showed that the produced suspension contained particles in the ~100 nm to 10 µm size range, with 1.0 - 2.0 µm on average, which is about 10 times smaller than the size of the initial material. FTIR spectroscopic investigations demonstrated that the chemical composition was preserved, while XRD and calorimetric measurements indicated partial amorphization of meloxicam during the process. The overall results suggest that the particles are mostly produced by the fragmentation of the pressed target by the recoil forces of the ablating laser pulse. Long period sedimentation tests of the suspension combined with UV-Vis spectroscopic analysis showed that by the method of PLAL a greater fraction of the poorly water soluble meloxicam could be dispersed and dissolved in water in a pharmaceutically preferred formation than by simple dissolution of it.

Keywords

Laser ablation; laser fragmentation; particle-size reduction; meloxicam; suspension

1. Introduction

Pulsed laser ablation (PLA) of different materials is a well-known process being used in several applications, especially on the field of material processing. It is extensively used for the micro-machining of various inorganic and organic samples. Main application areas include the construction of given patterns, surface structures, micro-objects (by direct etching), and the fabrication of thin layers (by collection of the ablated fragments onto a substrate surface (PLD)).

Several studies have already proved that PLA is suitable for the generation of micrometer- and submicrometer-sized particles from a wide range of materials in vacuum or gas environment. It has been demonstrated that by pulsed laser irradiation of iron target in water, iron-oxide particles can be formed at the liquid–solid interface [1]. Pulsed laser ablation in liquid (PLAL) is proved to be a promising route to produce clean colloids without any residual species in the case of metallic targets [2]. In the early 2000s PLAL became a well-established technique for the controlled fabrication of various nanoparticles (NPs) [3-5] for industrial, medical, biological or scientific research applications [6-10]. Thanks to the consistent and complementary theories and models, the process of PLAL is thoroughly described, and the method is reliably applicable for industrial NP fabrication [11-16].

In the beginning, PLAL has mainly been used to produce inorganic nanoparticles, such as diamond [17], metals and metal alloys [18-27], oxides [28-31] and semiconductor nanoparticles [32]. However, subsequent studies have shown that PLAL is also suitable for the production of organic nanoparticles, even though organic materials are more sensitive to optical radiation [33-39]. The obtained colloidal solution showed long time stability, typically for weeks or more, without the need of any additional surfactants due to the persistent Brownian motion of the nanoparticles in the solvent [37]. The size of the nanoparticles can be controlled by the experimental conditions such as the irradiating laser fluence [40,41], laser pulse duration [42] and wavelength [36]. The easy and high collectability of the created nanoparticles is a useful characteristic of laser ablation in the liquid phase.

Initially, only a few, less-sensitive organic materials were applied for nanoparticle generation by PLAL, however in the last decade several studies presented successful NP production from different organic matters, like vanadyl phthalocyanine, quinacridone, melamine cyanurate, polyethylene terephtalate, beclomethasone dipropionate [35,37,43-48]. It has been shown that both micron-sized (1 to 10 µm) and submicron-sized (400 to 900 nm) paclitaxel and megestrol acetate particles can be produced successfully by PLAL [45,46].

One of the most important application fields of organic NPs is pharmacology. Smaller drug particles have higher surface to volume ratio, and therefore they have improved dissolution rate and transport characteristics, which greatly assist their fast absorption and uptake by the human cells [49,50]. It has also been shown that the amorphization of pharmaceuticals can further improve their dissolution properties since in the amorphous form there is no need to take over the crystal lattice binding energies during the dissolution process. PLAL could be a non-conventional approach in drug formulation, as a simple, clean (no additional chemicals are needed) and rapid wet grinding method. The medical applicability of a drug nanosuspension produced by PLAL strongly depends on the attained size of the suspended particles. For example the best uptake of the poorly water-soluble oral and parenteral drugs can be achieved in the form of nanoparticles. For the intranasal and pulmonary application decreased size is a determinant factor. As pulmonary drugs, particles in the size range of 0.5 µm - 5 µm are the best absorbed in the lungs. Particles bigger than 5 µm are eliminated by the mucociliary clearance and can’t penetrate deep into the lungs, while, particles smaller than 0.5 µm are easily exhaled and also poorly absorbed [51]. Therefore, it is of particular interest to evaluate the size range of pulmonary drug particles prepared by PLAL.

In this paper pulsed laser ablation of a poorly water-soluble material, meloxicam, was investigated in water. Meloxicam is a nonsteroidal anti-inflammatory analgesic and antipyretic drug (NSAID), and it is frequently used to treat rheumatoid arthritis, osteoarthritis and other joint diseases [52]. However, meloxicam has low solubility at physiological pH which impedes its

clinical application. We studied the direct effect of laser fragmentation on the size decreasing and structural character of meloxicam, which is a potential model drug for our further nanosuspension formulations. The motivation of our study is to introduce a novel preparation method in drug preformulation and also to produce intermediate products for per os, nasal and pulmonary drug administration.

2. Materials

Meloxicam (4-hydroxy-2-methyl-N-(5-methyl-2-thiazolyl)-2H-benzothiazine-3-car-boxamide-1,1-dioxide) was obtained from EGIS Ltd., (Budapest, Hungary). It is a yellow powder with 10-50 µm average particle size, 100% crystalline.

3. Experimental methods

3.1. Preparation of nanosuspension by pulsed laser ablation in liquid

A frequency doubled Q-switched Nd:YAG laser beam (FWHM = 8 ns, λ = 532 nm, f = 3 Hz) was focused by a fused silica lens (f=10 cm) onto a target placed in a rotating water-containing vessel. The targets were pastille pressed from commercially available meloxicam powder by a hydraulic compactor at 175 MPa pressure. The applied laser fluences were varied between 4.2 – 9.4 J/cm^2 and the number of pulses was 48600. The meloxicam pastilles were placed in 20 ml distilled water (approximately 1.5 cm deep below the water surface) and clamped to the bottom of the vessel. In order to be treated evenly, the target was rotated under the beam during laser irradiation.

3.2. Size and morphology studies

After ablation an aliquot was taken from the solution, by avoiding the bottom of the vessel, in order to exclude pieces originating from occasional cracking and breaking of the surface layer of the pastille in consequence of the ablation induced mechanical forces. This step was important because these pieces could falsify the results of the investigations. Small droplets taken from the middle of the produced suspension were placed on silicon plates and left to dry for scanning electron microscopy investigations (SEM, Hitachi S-4700). Prior to imaging the samples were gold coated with a sputter coater (Bio-Rad SC 502). SEM images of some typical areas were recorded at different magnifications and analyzed using the ImageJ software.

3.3. Structural characterization

FTIR
For chemical characterization, the ablated particles were analyzed by Fourier transform infrared spectroscopy (FTIR). A portion of the suspension was taken from the middle of the vessel, right after the ablation. A few mg ablated particles were obtained from the suspension by the evaporation of water at 60°C. Then this dry powder was ground with 150 mg KBr in an achate mortar and the mixture was pressed to a self-supporting disk for the FTIR analysis.
FT-IR spectra were recorded with an FT-IR spectrometer (Thermo Nicolet AVATAR 330, LabX Midland, ON, Canada) between 4000 and 400 cm^{-1}, at a resolution of 4 cm^{-1}.

XRPD
Crystallinity of the dried meloxicam sample was characterized using an X-ray powder diffraction (XRPD) BRUKER D8 Advance X-ray diffractometer (Bruker AXS GmbH, Karlsruhe, Germany). The powder samples were loaded in contact with a plane quartz glass sample slide with an etched square. Cu-K$_{\alpha 1}$ radiation (λ = 1.5406 Å) source and a slit-detector was applied . Settings were as follows: the samples were scanned at 40 kV and 40 mA and the angular range was 3° to 40° 2θ, at a

step time of 0.1 s and a step size of 0.007°. The crystallinity index was calculated on the basis of the following formula: $A_{cryst}/(A_{cryst}+A_{amorph})$, where A_{cryst} and A_{amorph} denotes the area under the crystalline and amorphous peaks in the diffractogram, respectively.

MDSC

Differential scanning calorimetry (DSC) measurements were carried out on a TA Q20 (TA Instruments, USA) to examine and compare the thermal response of the ablated meloxicam with the original drugs'. The meloxicam powder was weighed into a Tzero aluminum sample pan and sealed with an aluminum Tzero lid. During modulated DSC (MDSC) measurements the samples were heated from 25 °C to 300 °C at a heating rate of 5°C/min with a temperature modulation of ±1°C in 60 seconds periods, in inert atmosphere. Results were analyzed by Universal Analysis V4.5 software.

3.4. Sedimentation test (dissolution of meloxicam)

The sedimentation of the ablated meloxicam particles in the aqueous medium was studied by extinction spectroscopy. The meloxicam suspension was produced by 43200 ablating laser pulses at 9.4 J/cm^2 fluence and the suspension was immediately transferred to a Shimadzu UV-2101PC VUV-Vis spectrophotometer. Extinction spectra were recorded repeatedly with time.

4. Experiments and results

4.1. Particle size distribution investigations

We compared the size distribution of the PLAL produced and the original meloxicam particles. Fig. 1. illustrates the evaluation process for the particles generated with PLAL and the reference powder. The ImageJ software calculated the area of each patch being assigned to the individual particles, and determined the diameter of a hypothetical sphere which would have the same projected area. This diameter value will be considered as the size of the corresponding particle. Since only a small mass fraction of particles were smaller than 200 nm, a lower limit of 100 nm for the measured particle size was set.

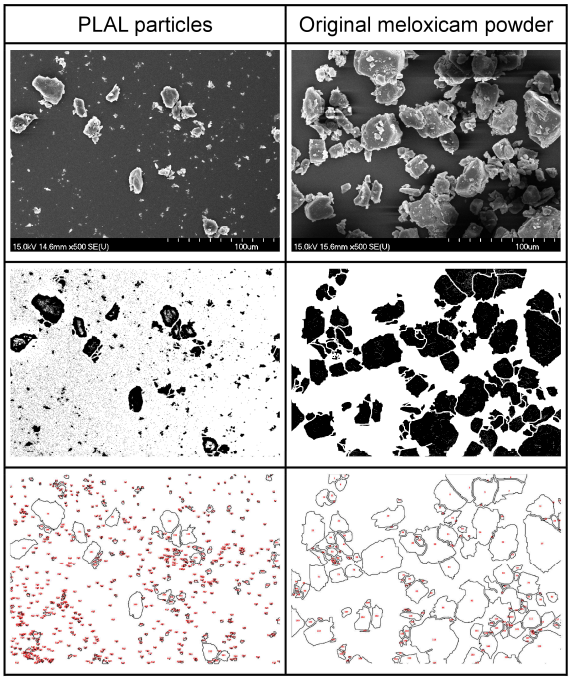

Fig. 1. *Steps for determination of the particle size distribution from SEM images using image processing software (for details see text).*

Fig. 2. shows, that while the particles of the original meloxicam are in the 2-35 µm size range, all of the particles obtained from the laser generated meloxicam suspension are smaller than 10 µm, and a significant fraction is in the sub-micrometer size range. We have to note, that the overlapping of particles observed especially for the original meloxicam powder can affect the calculated average size of the particles to some extent, but not decisively. The average dimensions of the meloxicam particles produced by PLAL at 9.4, 5.4 and 4.2 J/cm^2 fluences were calculated to be 1.33, 1.05 and 1.9 µm, respectively, while the original meloxicam powder particles were 16.5 µm on average size.

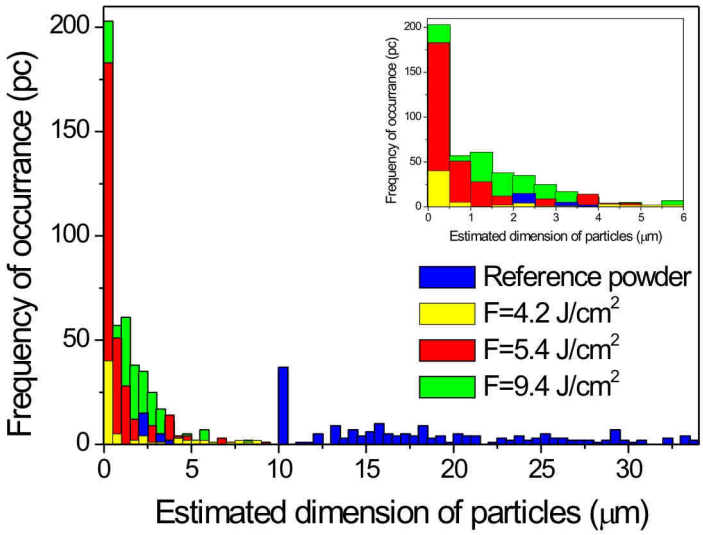

Fig. 2. *The size distribution of particles produced by ablation of meloxicam pastilles in water at different laser fluences. The original meloxicam powder was also investigated as reference.*

4.2. Morphological investigations

Small droplets of the suspensions produced by different laser fluences were placed on silicon plates and left to dry for scanning electron microscopy (SEM) investigations and for comparison with the original meloxicam powder (Fig. 3(a)-(c)). The particles of the raw meloxicam powder were ~2-40 µm in size and displayed a lamellar crystalline structure, with sharp edges (Fig.3(c)). The particles obtained from the ablation suspension were ~100 nm - 10 µm in size and less crystalline-like, having more rounded edges and showing traces of melting (Fig. 3(a),(b)). The morphology of the particles created at different laser energy densities was similar.

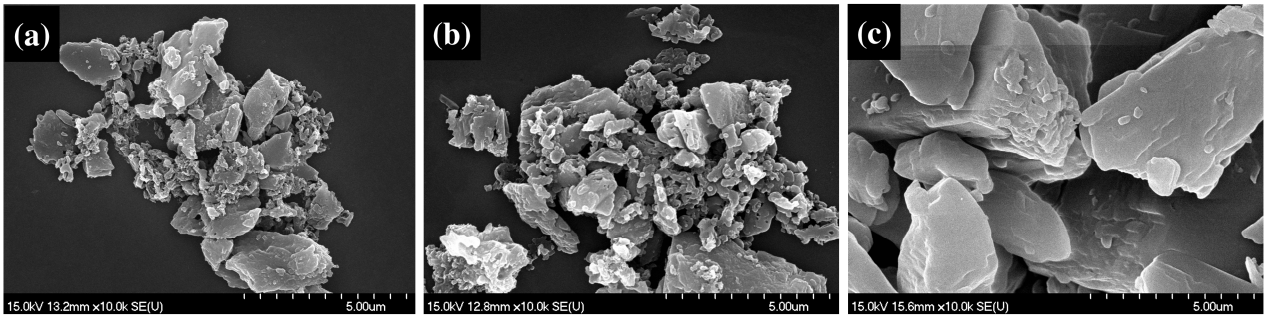

Fig. 3. *SEM images of the particles obtained from the meloxicam nanosuspension produced by (a) 4.2 J/cm^2 and (b) 9.4 J/cm^2 laser fluences and of the original meloxicam powder particles (c).*

4.3. Chemical composition and structural analysis

Our size-distribution measurements proved that the applied PLAL method is suitable for the particle size reduction. However, the chemical composition and crystal structure of the obtained particles are also important parameters for their pharmaceutical availability.

FTIR

The FTIR spectra showed no visible differences between the ablation produced particles and the original meloxicam powder in the investigated fluence range. Examining the fingerprint region (400 – 1700 cm^{-1}) the characteristic peaks matched to the reference (Fig. 4.). This indicates that the PLAL produced particles with reduced average size are chemically identical with the initial meloxicam.

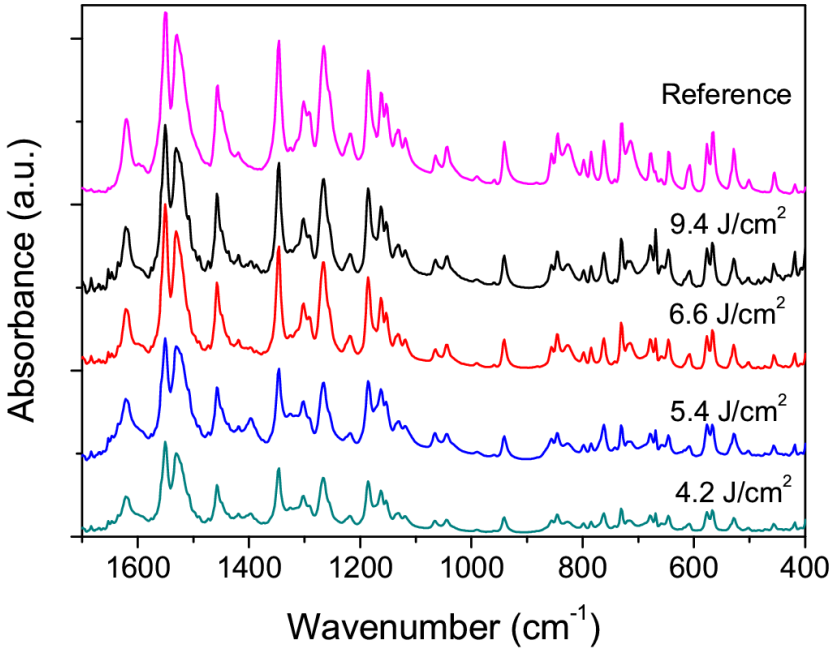

Fig. 4. *FTIR spectra of the particles generated by ablation in distilled water milieu at different laser fluences and the original meloxicam powder as reference.*

XRPD

The XRPD pattern of meloxicam particles produced by PLAL (Fig. 5.),was relatively weak, probably due to the small amount of sample available for the analysis, however the characteristic peaks of the original meloxicam powder were present at diffraction angles 2Θ of 13.22, 15.06, 26.46 and 26.67°, indicating their identical crystalline structure [54]. According to the crystallinity index calculation the ablated particles have 93,3% crystalline fraction.

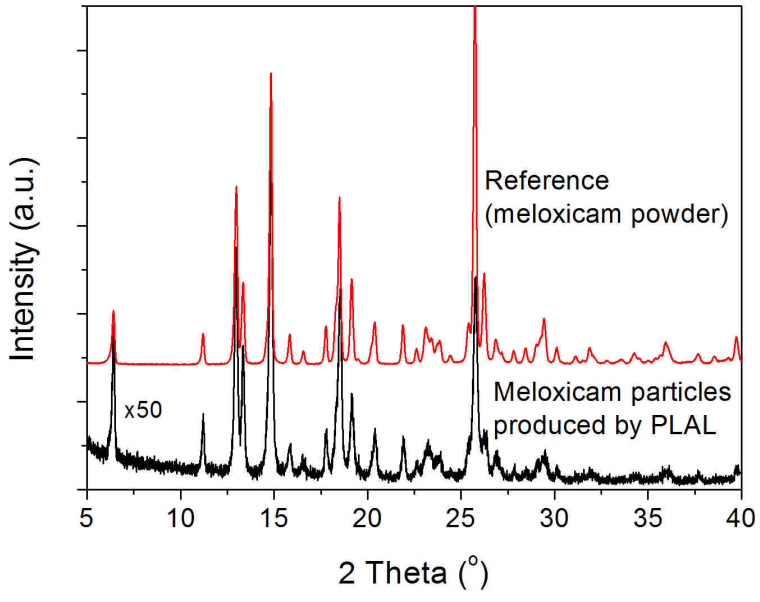

Fig.5.: XRPD pattern of meloxicam particles produced by PLAL compared to the reference meloxicam powder.

MDSC

As shown in Fig. 6. the melting point of the particles produced by laser ablation shifted to lower temperature (236 °C) as compared to the original crystalline meloxicam (258 °C). Earlier studies showed that this could be attributed to the amorphization of meloxicam to some degree [54, 55], which in our case can be the consequence of the laser treatment/fragmentation.

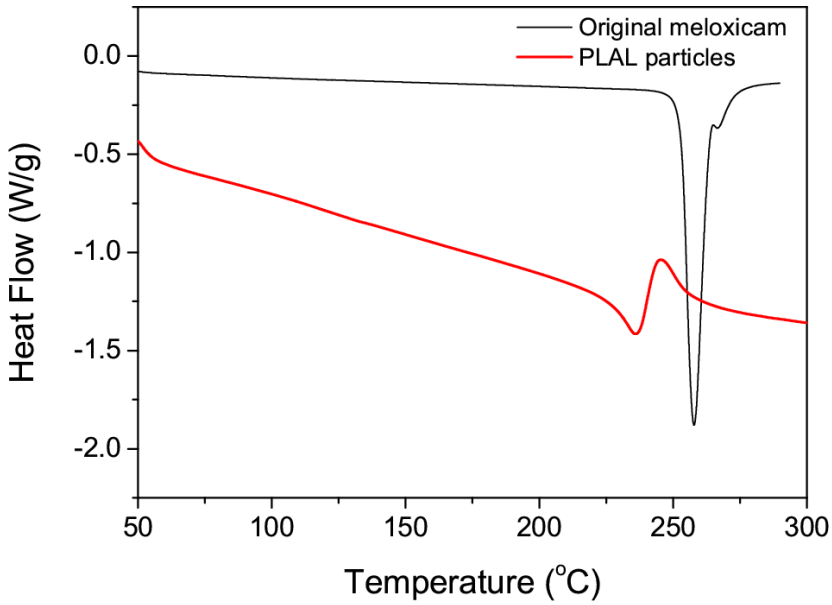

Fig. 6. *MDSC data of the particles produced by PLAL as compared to untreated meloxicam powder.*

4.4 Sedimentation test

For the medical application of the meloxicam suspension it is important to know the stability of the colloid solution produced by PLAL.

Extinction spectra were recorded at different times after the ablation (Fig. 7(a)). The intensity of the main meloxicam peak (at 360 nm) was plotted as a function of time (Fig. 7(b)). Over a 100 hour period it was found that the intensity of this peak first decreases, reaches a minimum value and then, after ~50 hours, it starts to increase again until it reaches its final value after ~90 hours. We suppose that during the time period of inspection two simultaneous processes, sedimentation and dissolution, occur and influence the extinction oppositely: i) in the beginning the relatively fast sedimentation of meloxicam particles results in the decrease of the extinction (mainly via the elimination of scattering sources from the bulk) ii) later on the relatively slow (and weak) chemical dissolution of meloxicam causes the slow increase of the extinction.

The analytical balance measurement showed that the ablation entailed a 3.5 mg loss in mass of the target pastille. This means that the produced suspension contains totally 3.5 mg meloxicam in 20 ml water in the form of particles and dissolved molecules. A reference suspension was made by adding 3.5 mg meloxicam powder to 20 ml distilled water and shacked for 2 minutes in ultrasonic bath. The extinction of the reference suspension was very low, and only a slight increase in it could be observed with time (Fig. 7(b)). The low initial extinction is attributed to the very small fraction of the particles floating in the bulk: most of the meloxicam powder is settled at the bottom of the cuvette or afloat on the surface of the water. After about 60 hours the extinction started to increase and then reached a constant value, indicating first the dissolution of meloxicam and then the saturation of the solution. (The solubility of meloxicam in water is 7.15 mg/L at 25°C [53].)

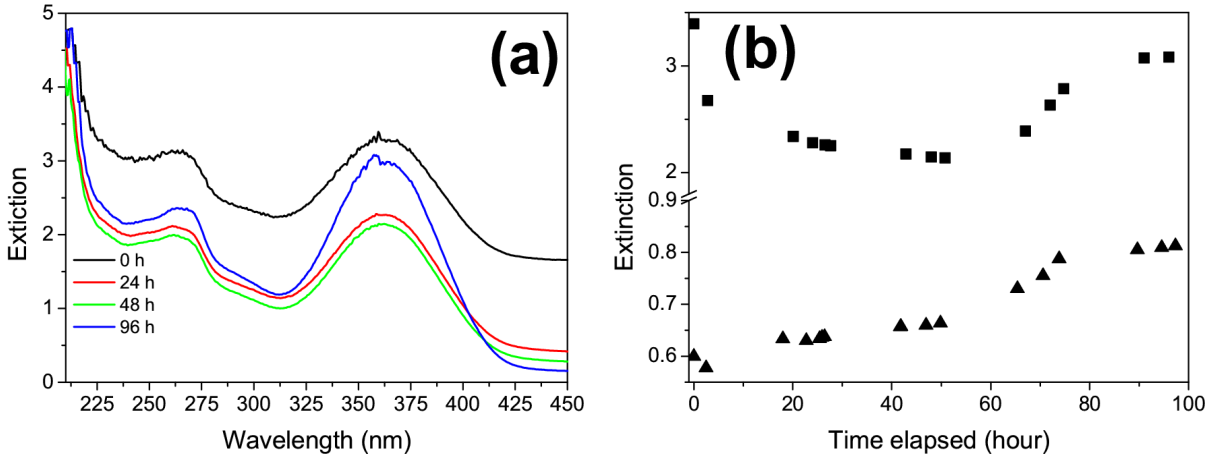

Fig. 7. *The extinction spectra of meloxicam suspension produced by 9.4 J/cm^2 ablating fluence at different times elapsed (a). Graph (b) shows the intensity of the main meloxicam peak (at 360 nm) as a function of time for the PLAL generated (■) and reference solution (▲). Note the different scaling above and below the axis brake in (b).*

5. Discussion

The absorption of laser photons in the surface layer of meloxicam pastille can result in thermal dissociation of the molecules. Thermal model calculations were carried out to estimate the temperature of the uppermost surface layer of the pastille after one laser pulse. We applied the Lambert-Beer law in order to estimate the temperature change as the function of depth by neglecting the heat conduction:

$$\Delta T(x) = \frac{\alpha \cdot F}{\rho \cdot c} \cdot e^{-\alpha x},$$

where α is the absorption coefficient at 532 nm, ρ is the density, c is the specific heat of meloxicam and F is the applied laser fluence. Due to lack of data in the literature, the absorption coefficient of meloxicam was determined by ellipsometry, which resulted in α=4 μm^{-1}. For the mean specific heat of meloxicam in the temperature range 25-250 °C (*i.e.*, below the decomposition temperature) we obtained 1800 J/(kgK) on the basis of Modulated Heat Flow measurement by Modulated Differential Scanning Calorimetry (MDSC). The thermal decomposition temperature of meloxicam was measured to be 258.7 °C, in good agreement with the data in PubChem open chemistry database (254 °C) [53].

Our thermal model calculation demonstrated that the temperature of the upper 227-429 nm layer of the pastille exceeds the decomposition temperature of meloxicam in the whole range of laser fluence (4.2-9.4 J/cm^2) applied. It is plausible that the fast decomposition of meloxicam molecules in the uppermost volume element gives rise to an explosion-like gas emission and expansion (Fig. 8(a)-(c)). The generated recoil forces tear off and accelerate softened/molten droplets and solid particles from the bottom of the ablation hole into the solution pulse by pulse (Fig. 8(c)-(d)). Thereby, a meloxicam suspension is formed. The typical size of the ejected grains ranges from tens of nanometers to a few micrometers, while the even smaller particles tend to aggregate and form larger particles.

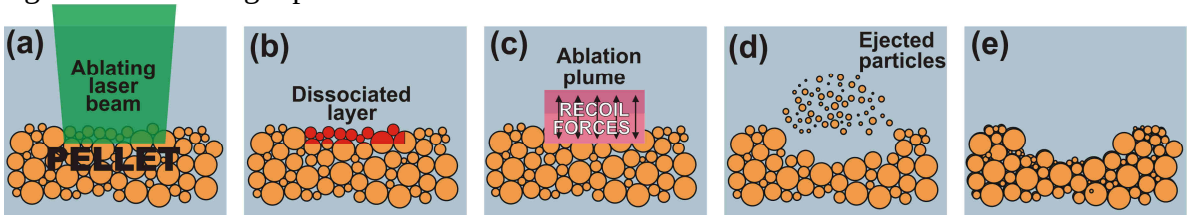

Fig. 8. *Phenomenological model of the particle generation process during laser ablation of meloxicam pastille.*

SEM images of the ablated area demonstrate that a significant amount of micrometer- to sub-micrometer-size debris can be found at the bottom of the ablation hole (Fig. 9(a)). At larger magnifications re-solidified molten droplets and jets can also be seen in the ablated area (Fig. 9(b)). Figures (c) and (d) show the pressed (intact upper surface) and the fracture surface of the original meloxicam pastille, respectively.

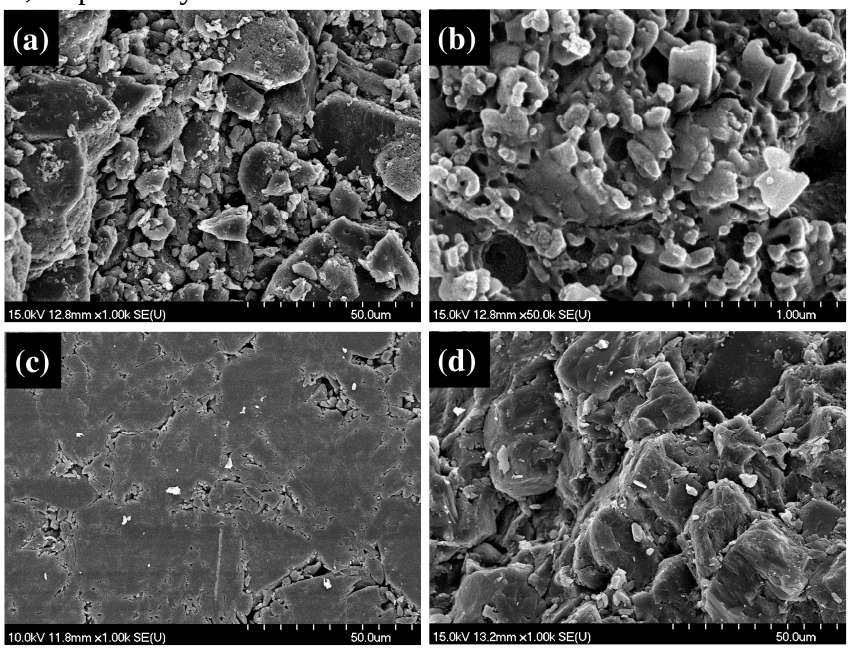

Fig. 9. *SEM images (a) and (b) of the bottom of a laser ablated hole (F= 5.4 J/cm^2), captured at different magnifications. Solid debris (a) and re-solidified molten droplets and jets (b) can be seen well. As reference, the pressed (c) and the fracture (d) surface of the original meloxicam pastille is shown.*

6. Conclusion

PLAL has been applied successfully for the production of highly stable aqueous suspension of near-micrometer size meloxicam particles.

The average size of the particles produced by 532 nm laser ablation of meloxicam pastilles fell in the 1.0 - 2.0 µm range. This is approximately one tenth of the average size of the original meloxicam powder particles (16.5 µm) and thereby it is more appropriate for the cellular uptake of the drug.

We established that the ablated particles were chemically identical with the original meloxicam powder for all applied laser fluences.

According to our observations, a fast sedimentation of the big particles occurs in the suspension during the first two days and after about 50 hours only the slow chemical dissolution of meloxicam can be seen. The higher extinction of the ablated suspension as compared to the reference meloxicam suspension during the whole time period of observation indicates that a larger amount of small particles could be dispersed in water by PLAL than by the simple dissolution of the original powder of the drug. The sedimentation measurements proved the stability of the PLAL produced suspension over a 100 hour time period as well.

Our thermo-mechanical model calculations predicted that each laser pulse triggers the explosive decomposition of the target molecules in the upper 227-429 nm layer. The fast expansion of this upper volume element results in significant mechanical forces in its close proximity which can tear out meloxicam particles from the target pastille. The particles being ablated into the solvent on this (“gentle”) way suffer no chemical decomposition but still are much smaller than the particles of the original meloxicam powder.

The crystal structure of meloxicam didn't change during the ablation process, and only a slight decrease in the crystalline fraction was observed. The amorphization of meloxicam could also increase the dissolution rate and improve the bioavailability of the poorly water soluble drug (especially if accessing the nanometer size range as well) [55].

On the basis of our results we can conclude that pulsed laser ablation of meloxicam pastille in water is appropriate for the preparation of pure meloxicam suspension. The obtained size range of the particles predicts that PLAL may become a superior technique for the production of intermediate products for per os, nasal and pulmonary drug administration.

Acknowledgement This work was supported by the GINOP-2.3.2-15-2016-00036 ("Development and application of multimodal optical nanoscopy methods in life and materials sciences") project.

References

1 Patil PP, Phase DM, Kulkarni SA, Ghaisas SV, Kulkarni SK, Kanetkar SM, Ogale SB and Bhide VG 1987 Pulsed-laser-induced reactive quenching at liquid-solid interface: Aqueous oxidation of iron *Phys. Rev. Lett*. **58**, 238-41. doi:10.1103/PhysRevLett.58.238.
2 Neddersen J, Chumanov G and Cotton TM 1993 Laser Ablation of Metals: A New Method for Preparing SERS Active Colloids *Appl. Spectrosc.* **47**, 1959-64. doi:10.1366/0003702934066460.
3 Mafune F, Kohno J, Takeda Y, Kondow T and Sawabe H 2000 Formation and size control of sliver nanoparticles by laser ablation in aqueous solution *J. Phys. Chem. B* **104,** 9111-17. doi:10.1021/jp001336y.
4 Yan ZJ and Chrisey DB Pulsed laser ablation in liquid for micro-/nanostructure generation 2012 *Journal of Photochemistry and Photobiology C- Photochemistry Reviews* **13**, 204-23. doi:10.1016/j.jphotochemrev.2012.04.004.
5 Besner S and Meunier M 2010 Laser Synthesis of Nanomaterials. In: Sugioka K, Meunier M, Piqué A, editors. Laser Precision Microfabrication, Berlin, Heidelberg: Springer Series in Materials Science, Springer. doi: 10.1007/978-3-642-10523-4_7.
6 Brigger I, Dubernet C and Couvreur P 2002 Nanoparticles in cancer therapy and diagnosis *Adv. Drug Deliv. Rev.* **54**, 631-51. doi:10.1016/S0169-409X(02)00044-3.
7 Katz E and Willner I 2004 Integrated nanoparticle-biomolecule hybrid systems: Synthesis, properties, and applications *Angew. Chem.* **43,** 6042-108. doi:10.1002/anie.200400651.
8 Luo X, Morrin A, Killard AJ and Smyth MR 2006 Application of nanoparticles in electrochemical sensors and biosensors *Electroanalysis* **18**, 319-26. doi:10.1002/elan.200503415.
9. Xiao Y, Patolsky F,. Katz E, Hainfield JF and Willner I 2003 "Plugging into enzymes": Nanowiring of redox enzymes by a gold nanoparticle *Science* **299**, 1877-81. doi:10.1126/science.1080664.
10 Oberdörster G, Oberdörster E and Oberdörster J 2005 Nanotoxicology: An emerging discipline evolving from studies of ultrafine particles *Environ. Health Perspect.* **113**, 823-39. doi:10.1289/ehp.7339.
11 Dell'Aglioa M, Gaudiusoa R, De Pascale O and De Giacomo A 2015 Mechanisms and processes of pulsed laser ablation in liquids during nanoparticle production *Appl. Surf. Science* **348**, 4-9. doi:10.1016/j.apsusc.2015.01.082.
12 Barcikowski S, Devesa F and Moldenhauer K 2009 Impact and structure of literature on nanoparticle generation by laser ablation in liquids *J. Nanopart. Res.* **11**, 1883–1893. doi:10.1007/s11051-009-9765-0.
13 Barcikowski S and Compagnini G Advanced nanoparticle generation and excitation by lasers in liquids 2013 *Phys. Chem. Chem. Phys.* **15,** 3022-3026. doi:10.1039/c2cp90132c.
14 Yang G editor. Laser ablation in liquids: principles and applications in the preparation of nanomaterials 1st ed 2012 Singapore:Pan Stanford Publishing Pte.Ltd.

15 Amendola V and Meneghetti M What controls the composition and the structure of nanomaterials generated by laser ablation in liquid solution? 2013 *Phys Chem Chem Phys* **15,** 3027-46. doi:10.1039/c2cp42895d.
16 Guo D, Xie G and Luo J 2014 Mechanical properties of nanoparticles: basics and applications *J. Phys. D.-Appl Phys.* **47**, 013001. doi:10.1088/0022-3727/47/1/013001.
17 Yang GW and Wang JB 2000 Carbon nitride nanocrystals having cubic structure using pulsed laser induced liquid-solid interfacial reaction *Appl. Phys. A.* **71**, 343-44. doi:10.1007/s003390000590.
18 Compagnini G, Scalisi A and Puglisi O 2002 Ablation of noble metals in liquids: a method to obtain nanoparticles in a thin polymeric film *Phys. Chem. Chem. Phys.* **4**, 2787-91. doi:10.1039/b109490d.
19 Dolgaev SI, Simakin AV, Voronov VV, Shafeev GA and Bozon-Verduraz F 2002 Nanoparticles produced by laser ablation of solids in liquid environment *Appl. Surf. Sci.* **186**, 546-551. doi:10.1016/S0169-4332(01)00634-1.
20 Compagnini G, Scalisi A, Puglisi O and Spinella C Synthesis of gold colloids by laser ablation in thiol-alkane solutions 2004 *J. Mater. Res.* **19**, 2795-98. doi:10.1557/jmr.2004.0401.
21 Simakin AV, Voronov VV, Kirichenko NA and Shafeev GA Nanoparticles produced by laser ablation of solids in liquid environment 2004 *Appl. Phys. A* **79**, 1127-32. doi:10.1007/s00339-004-2660-8.
22 Zeng HB, Cai WP, Li Y, Hu JL and Liu PS 2005 Composition/structural evolution and optical properties of ZnO/Zn nanoparticles by laser ablation in liquid media *J. Phys. Chem. B* **109**, 18260-6. doi:10.1021/jp052258n.
23 Yeh MS, Yang YS, Lee YP, Lee HF, Yeh YH and Yeh CS 1999 Formation and Characteristics of Cu Colloids from CuO Powder by Laser Irradiation in 2-Propanol *J. Phys. Chem. B*: **103,** 6851-57. doi: 10.1021/jp984163+.
24 Shafeev GA, Freysz E and Bozon-Verduraz F Self-influence of a femtosecond laser beam upon ablation of Ag in liquids 2004 *Appl. Phys. A* **78**, 307-9. doi:10.1007/s00339-003-2357-4.
25 Sylvestre JP, Poulin S, Kabashin AV, Sacher E, Meunier M and Luong JHT 2004 Surface chemistry of gold nanoparticles produced by laser ablation in aqueous media *J Phys Chem B* **108**, 16864-69. doi:10.1021/jp047134+.
26 Dobbins TA, Poondi D and Singh J 1999 Synthesis of micron and submicron nickel and nickel oxide particles by a novel laser-liquid interaction process *J. Mater. Synth. Process.* **7**, 261-71. doi:10.1023/A:1021864719176.
27 Poondi D and Singh J 2000 Synthesis of metastable silver-nickel alloys by a novel laser-liquid-solid interaction technique *J. Mater. Sci.* **35**, 2467-76. doi:10.1023/A:1004765618078.
28 Ryu JH, Park GS, Kim KM, Lim CS, Yoon JW and Shim KB 2007 Synthesis of $CaWO_4$ nanocolloidal suspension via pulsed laser ablation and its optical properties *Appl. Phys. A* **88**, 731-6. doi:10.1007/s00339-007-4051-4.
29 Sugiyama M, Okazaki H and Koda S 2002 Size and shape transformation of TiO_2 nanoparticles by irradiation of 308-nm laser beam *Jpn. J. Appl. Phys.* **41**, 4666-74. doi:10.1143/JJAP.41.4666.
30 Tsuji T, Hamagami T, Kawamura T, Yamaki J and Tsuji M 2005 Laser ablation of cobalt and cobalt oxides in liquids: influence of solvent on composition of prepared nanoparticles. *Appl. Surf. Sci.* **243**, 214-19. doi:10.1016/j.apsusc.2004.09.065.
31 Chen JW, Dong QZ, Yang J, Guo ZX, Song ZL and Lian JS 2004 The irradiation effect of a Nd-YAG pulsed laser on the CeO_2 target in the liquid *Mater. Lett.* **58**, 337-41. doi:10.1016/S0167-577X(03)00482-8.
32 Ankin KV, Melnik NN, Simakin AV, Shafeev GA, Voronov VV and Vitukhonovsky AG 2002 Formation of ZnSe and CdS quantum dots via laser ablation in liquids *Chem. Phys. Lett.* **366**, 357-60. doi:10.1016/S0009-2614(02)01534-8.
33 Volkov VV, Asahi T, Masuhara H, Masuhara A, Kasai H, Oikawa H, *et al*. 2004 Size-dependent optical properties of polydiacetylene nanocrystal *J. Phys. Chem. B* **108**, 7674-7680. doi:10.1021/jp031369o.

34 Tamaki Y, Asahi T and Masuhara H 2000 Tailoring nanoparticles of aromatic and dye molecules by excimer laser irradiation. *Appl. Surf. Sci.* **168**, 85-8. doi:10.1016/S0169-4332(00)00596-1.
35 Tamaki Y, Asahi T and Masuhara H 2001 Nanoparticle formation of vanadyl phthalocyanine by laser ablation of its crystalline powder in a poor solvent *J. Phys. Chem. A* **106**, 2135-2139. doi:10.1021/jp012518a.
36 Sugiyama T, Asahi T, Takeuchi T and Masuhara H 2006 Size and phase control in quinacridone nanoparticle formation by laser ablation in water *Jpn. J. Appl. Phys.* **45**, 384-8. doi:10.1143/JJAP.45.384.
37 Asahi T, Sugiyama T and Masuhara H 2008 Laser fabrication and spectroscopy of organic nanoparticles *Acc. Chem. Res.* **41**, 1790-8. doi: 10.1021/ar800125s.
38 Yasukuni R, Asahi T, Sugiyama T, Masuhara H. Sliwa M, Hofkens J, *et al*. 2008 Fabrication of fluorescent nanoparticles of dendronized perylenediimide by laser ablation in water. *Appl. Phys. A* **93**, 5-9. doi:10.1007/s00339-008-4661-5.
39 Yasukuni R, Sliwa M, Hofkens J, C. De Schryver F, Herrmann A, Muellen K and Asahi T 2009 Size-dependent optical properties of dendronized perylenediimide nanoparticle prepared by laser ablation in water *Jpn. J. Appl. Phys.* **48**, 065002.
40 Tabata H, Akamatsu M, Fujii M and Hayashi S 2007 Formation of C_{60} colloidal particles suspended in poor solvent by pulsed laser irradiation *Jpn J Appl Phys* **46**, 4338-43. doi:10.1143/JJAP.46.4338.
41 Hahn A, Barcikowski S and Chichkov BN 2008 Influences on Nanoparticle Production during Pulsed Laser Ablation *JLMN-Journal of Laser Micro/Nanoengineering* **3**, 73-7. doi:10.2961/jlmn.2008.02.0003.
42 Zhigilei LV and Garrison BJ 2000 Microscopic mechanisms of laser ablation of organic solids in the thermal and stress confinement irradiation regimes *J. Appl. Phys.* **88**, 1281-97. doi:10.1063/1.373816.
43 Hobley J, Nakamori T, Kajimoto S, Kasuya M, Hatanaka K, Fukumura H, *et al*. 2007 Formation of 3,4,9,10-perylenetetracarboxylicdianhydride nanoparticles with perylene and polyyne byproducts by 355 nm nanosecond pulsed laser ablation of microcrystal suspensions *Journal of Photochemistry and Photobiology A: Chemistry* **189**, 105-13. doi:10.1016/j.jphotochem.2007.01.016.
44 Wagener P and Barcikowski S 2010 Laser fragmentation of organic microparticles into colloidal nanoparticles in a free liquid jet *Appl. Phys. A* **101**, 435-39. doi:10.1007/s00339-010-5814-x.
45 Kenth S, Sylvestre JP, Fuhrmann K, Meunier M and Leroux JC 2011 Fabrication of Paclitaxel Nanocrystals by Femtosecond Laser Ablation and Fragmentation *J. Pharm. Sci.* **100**, 1022-30. doi:10.1002/jps.22335.
46 Sylvestre JP, Tang M., Furtos A, Leclair G, Meunier M and Leroux JC 2010 Nanonization of megestrol acetate by laser fragmentation in aqueous milieu *J. Control. Release* **149**, 273-80. doi:10.1016/j.jconrel.2010.10.034.
47 Ding W, Sylvestre JP, Leclair G and Meunier M 2012 Laser Fragmentation as an Efficient Size-Reduction Method for Pulmonary Drug Discovery: Proof-of-Concept Study of Beclomethasone Dipropionate. *International Journal of Theoretical and Applied Nanotechnology* **1**, 99-104.
48 Elaboudi I, Lazare S, Belin C, Talaga D and Labrugère C 2008 From polymer films to organic nanoparticles suspensions by means of excimer laser ablation in water *Appl Phys A* **93**, 827-31. doi:10.1007/s00339-008-4746-1.
49 Mosharraf M and Nyström C 1995 The effect of particle size and shape on the surface specific dissolution rate of microsized practically insoluble drugs *International Journal of Pharmaceutics* **122**, 35-47. doi:10.1016/0378-5173(95)00033-F.
50 Rasenack N, Hartenhauer H and Muller B 2003 Microcrystals for dissolution rate enhancement of poorly water soluble drugs *International Journal of Pharmaceutics* **254**, 137-45. doi:10.1016/S0378-5173(03)00005-X.
51 Taylor K. Pulmonary drug delivery. In Aulton ME, editor. Aulton's Pharmaceutics: The Design and Manufacture of Medicines, 3rd ed 2007 Edinburgh: Churchill Livingstone.

52. Hanft G, Türck D, Scheuere, S and Sigmund R 2001 Meloxicam oral suspension: a treatment alternative to solid meloxicam formulations *Inflammation Research* **50**(Suppl 1), 35-7. doi:10.1007/PL00000219.
53 PubChem open chemistry database. Compound Summary for CID 54677470. https://pubchem.ncbi.nlm.nih.gov/compound/meloxicam
54 Freitas JTJ, Viana OMMS, Bonfilio R, Doriguetto AC and de Araujo MB 2017 Analysis of polymorphic contamination in meloxicam raw materials and its effects on the physicochemical quality of drug product *Eur. J. Pharm. Sci.* **109**, 347-58. doi:10.1016/j.ejps.2017.08.029.
55 Bartos Cs, Szabó-Révész P, Bartos Cs, Katona G, Jójárt-Laczkovich O and Ambrus R 2016 The Effect of an Optimized Wet Milling Technology on the Crystallinity, Morphology and Dissolution Properties of Micro- and Nanonized Meloxicam *Molecules* **21**(4), 507. doi:10.3390/molecules21040507.